Astron. Astrophys. 354, 1053–1061 (2000)

ASTRONOMY AND ASTROPHYSICS

ISO SWS-LWS observations of the prototypical reflection nebula NGC 7023⋆

A. Fuente[1], J. Martín-Pintado[1], N.J. Rodríguez-Fernández[1], J. Cernicharo[2], and M. Gerin[3]

[1] Observatorio Astronómico Nacional (IGN), Campus Universitario, Apdo. 1143, 28800 Alcalá de Henares (Madrid), Spain (fuente@oan.es)
[2] Instituto de Estructura de la Materia, Departamento de Física Molecular, CSIC, Serrano 121, 28006 Madrid, Spain
[3] DEMIRM, Observatoire de Paris, 61 Av. de l'Observatoire, 75014 Paris, France

Received 22 September 1999 / Accepted 24 December 1999

Abstract. We present SWS and LWS ISO observations towards a strip across the photodissociation region (PDR) in the reflection nebula NGC 7023. SWS02 and LWS01 spectra have been taken towards the star and the brightest infrared filaments located NW and SW from the star (hereafter NW and SW PDRs). In addition, SWS02 spectra have been taken towards two intermediate positions (NW1 and SW1). This has provided important information about the extent and spatial distribution of the warm H_2 and of the atomic species in this prototypical reflection nebula.

Strong emission of the [SiII] 34.8 μm line is detected towards the star. While all the PDR tracers (the [CII] 157.7 μm, [OI] 63.2 and 145.6 μm, [HI] 21cm and the H_2 rotational lines) present a ring-like morphology with the peaks toward the NW and SW PDRs and a minimum around the star, the SiII emission is filling the hole of this ring with the peak towards the star. This morphology can only be explained if the SiII emission arise in the lowest extinction layers of the PDR ($A_v < 2$ mag) and the HII region. At least 20% – 30% of the Si must be in gas phase in these layers. For $A_v \geq 2$ mag, the Si is mainly in solid form (δ Si = -1.3).

The NW and SW PDRs have very similar excitation conditions, high density filaments (n$\sim 10^6$ cm^{-3}) immersed in a more diffuse interfilament medium (n$\sim 10^4$ cm^{-3}). In both, the NW and SW PDRs, the intensities of the H_2 rotational lines can only be fitted by assuming an ortho-to-para-H_2 ratio lower than 3 in gas with rotation temperatures from 400 to 700 K. Therefore, there is a non-equilibrium OTP ratio in the region. Furthermore, the comparison between the OTP ratio derived from H_2 vibrational lines and the pure H_2 rotational lines, shows that the OTP ratio increases from $\sim$ 1.5 to 3 across the photodissociation region with larger values in the less shielded gas ($A_v < 0.7$ mag). This behavior is interpreted as a consequence of an advancing photodissociation front.

We have not detected the OH, CH and CH_2 lines towards the observed positions. This is consistent with the weakness of these lines in other sources and can be explained as a consequence of the small beam filling factor of the dense gas in the LWS aperture. The CO J=17→16 line has been tentatively detected towards the star.

Key words: stars: individual: HD 200775 – stars: pre-main sequence – ISM: abundances – ISM: individual objects: NGC 7023 – ISM: reflection nebulae – infrared: ISM: lines and bands

1. Introduction

NGC 7023 is a prototypical photodissociation region that has been largely studied in the last 10 years. It is a reflection nebula illuminated by the Herbig B3Ve star HD 200775. HD 200775 is located in a cavity of the molecular cloud whose sharp edges delineate perfectly the optical nebula (Fuente et al. 1992; Rogers et al. 1995; Fuente et al. 1998). Observations of CI and OII by Chokshi et al. (1988) reveal that a dense PDR is formed in the walls of this cavity with its peak located 50" NW from the star. Chokshi et al. (1988) carried out the first model for this region and estimated a UV field of $G_0(\lambda > 912$ Å)=2.4 10^3 in units of the Habing field and a density of n = 10^4 cm^{-3}. Because of its edge-on geometry and proximity (d $\sim$ 440 pc), this PDR turned out to be one of the best sites to study the physical and chemical processes taking place in a PDR. Fig. 1 shows the column density map of HI as derived from the [HI] 21 cm line superposed on the integrated intensity map of the ^{13}CO J=1→0 line. The HI peak is shifted $\approx$ 20 $''$ relative to the molecular ridge, showing the layered structure expected in a PDR (Fuente et al. 1998).

Very high angular resolution images of the region in the Extended Red Emission (ERE) and vibrationally excited H_2 lines show that the PDR has a filamentary structure with very bright thin filaments located 50$''$ NW and 70$''$ SW from the star (Sellgren et al. 1992; Lemaire et al. 1996). Hereafter, we will refer to these positions as NW PDR and SW PDR respectively. The NW PDR is spatially coincident with the peak of the CI and OII lines and has been extensively studied in atomic and molecular lines (Chokshi et al. 1988; Fuente et al. 1993, 1996;

⋆ Based on observations with ISO, an ESA project with instruments funded by ESA Member States (especially the PI countries France, Germany, the Netherlands and the United Kingdom) and with participation of ISAS and NASA

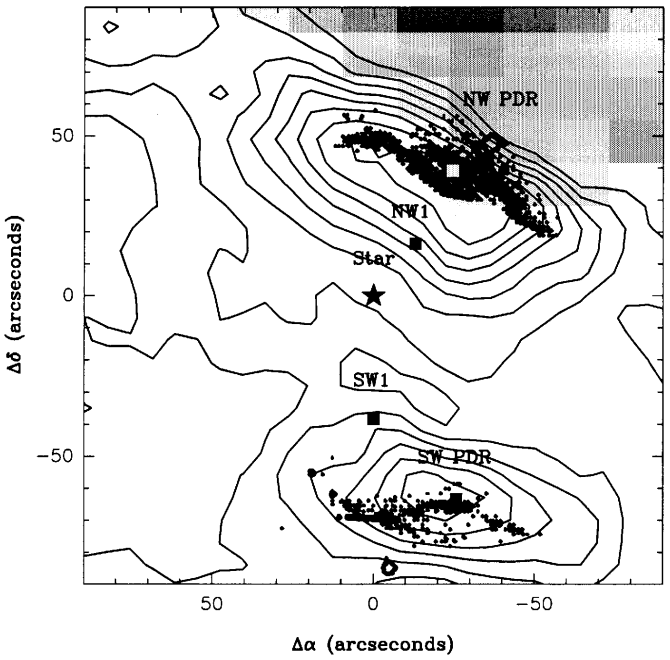

Fig. 1. Scheme of the observed region. The HI total column density map (contours) is superposed on the integrated intensity map of the ^{13}CO J=1→0 map (grey scale) (Fuente et al. 1998). The filaments observed in H_2 fluorescent emission are also shown (Lemaire et al. 1996). The observed positions are indicated by filled squares and the star.

Fuente & Martín-Pintado 1997; Lemaire et al. 1996, 1999; Martini et al. 1997; Gerin et al. 1998). Fuente et al. (1993) and Fuente & Martín-Pintado (1997) observed that the CN/HCN and CO^+/HCO^+ abundance ratios increases by a factor 10 and > 100 respectively towards this position relative to the values in the molecular cloud. Both, the CN/HCN and CO^+/HCO^+ abundance ratios are expected to increase in the lower extinction layers of PDRs (Fuente et al. 1993; Sternberg & Dalgarno 1995). An interferometric image of the HCO^+ line towards the NW PDR show that the PDR has also a filamentary structure in molecular emission with high density filaments ($n > 10^5$ cm^{-3}) embedded in a more diffuse medium ($n \sim 10^4$ cm^{-3}) (Fuente et al. 1996). The HCO^+ filaments are spatially coincident with the filaments seen in the near-infrared continuum images and in the emission of the vibrational H_2 lines.

The SW PDR is fainter by a factor 2-3 than the northern one and has been less studied in both, molecular and atomic lines. Gerin et al. (1998) reported observations of this PDR in CO and CI lines.

We have observed a strip which joins the NW PDR, the star and SW PDR using the SWS and LWS instrument on board of ISO. These observations have provided a very important information about the extent and spatial distribution of the warm H_2 and the atomic species within the PDR.

2. Observations

The observations were made using the Long- Wavelength Spectrometer (LWS) (Clegg et al. 1996; Swinyard et al. 1996) and the Short-Wavelength Spectrometer (SWS) (de Graauw et al. 1996) on board the Infrared Space Observatory (ISO) (Kessler et al. 1996). The LWS observations were carried out in full grating scan mode (LWS01 AOT) which provides coverage of the 43 - 90.5 μm range with a spectral resolution of 0.29 μm and of the 90.5 - 196.5 μm range with a resolution of 0.60 μm with ten independent detectors. Since the instrumental beam size is 74″ - 90″, we have observed only three positions of the nebula, the NW PDR, the star and the SW PDR. In Table 1, we give the coordinates of the observed positions. The data were processed using version 6 of the off-line pipeline (OLP V6). The uncertainty in the calibration is of about 30% (Swinyard et al. 1996)

We have observed one HI recombination line (Brα), five H_2 pure rotational lines (S(0),S(1),S(2),S(3), S(4) and S(5) v=0–0) and four ionic and atomic fine structure lines ([SIV] 10.5 μm, [FeII] 26.0 μm, [SIII] 33.5 μm and [SiII] 34.8 μm) using SWS AOT02. This mode provides a spectral resolution of $\lambda/\Delta\lambda \sim$ 1000-2000. All the observed lines are unresolved at this spectral resolution. The aperture of the instrument in these line ranges from 14″ x 20″ to 20″ x 33″. In order to study the spatial distribution of these lines we have observed 5 positions along the strip that joins the NW PDR, the star and the SW PDR. These positions are marked in Fig. 1, the observed spectra are shown in Fig. 2 and absolute coordinates are given in Table 1. Data reduction are carried out with version 7.0 of the Off Line Processing routines and the SWS Interactive Analysis at the ISO Spectrometer Data Center at the Max-Planck-Institut für Extraterrestrische Physik. The uncertainties in the calibration are of about 20% at short wavelengths (2 - 20 μm) and of about 30% at longer wavelengths (Salama et al. 1997).

Table 1. Observations

Position	Coordinates (2000)
NW PDR	$21^h01^m32^s.5$ 68°10′27″.5
NW1	$21^h01^m34^s.5$ 68°10′05″.0
Star	$21^h01^m36^s.9$ 68°09′48″.3
SW1	$21^h01^m36^s.9$ 68°09′10″.0
SW PDR	$21^h01^m32^s.3$ 68°08′45″.0

Table 2. Intensitites of the OI and CII lines

(x 10^{-4} erg s^{-1} cm^{-2} sr^{-1})	NW PDR	star	SW PDR
OI(63 μm)	7.5±0.1	3.9±0.8	3.8±1.3
OI(145.6 μm)	0.9±0.1	0.4±0.1	0.3±0.1
CII(157.7 μm)	2.8±0.1	1.8±0.1	1.7±0.1
OI(63 μm)/OI(145.6 μm)	8.3	9.0	12.7
OI(63 μm)/CII(157.7 μm)	2.7	2.2	2.3

3. Results

The LWS and SWS observational results are shown in Tables 2 and 3. The spectra of the SWS observations are shown in Fig. 2. In order to study the spatial distribution of the different lines,

Table 3. SWS observations

Line ($\times 10^{-5}$ erg s^{-1} cm^{-2} sr^{-1})	$\lambda(\mu m)$	NW PDR	NW1	Star	SW1	SW PDR
Recombination lines						
Brα	4.051	$\leq$2.3	$\leq$1.0	141.7$\pm$1.5	$\leq$0.7	$\leq$1.0
H_2 rotational lines						
H_2 S(5)	6.909	26.4$\pm$3.0	$\leq$4.8	$\leq$7.1	$\leq$3.3	9.2$\pm$3.3
H_2 S(4)	8.025	15.0$\pm$0.2	$\leq$3.9	$\leq$5.0	$\leq$1.4	5.6$\pm$1.1
H_2 S(3)	9.665	40.8$\pm$1.3	$\leq$4.4	$\leq$3.3	$\leq$1.6	21.2$\pm$1.5
H_2 S(2)	12.279	24.0$\pm$3.3	$\leq$10	$\leq$7.4	$\leq$8.0	16.5$\pm$2.7
H_2 S(1)	17.035	21.4$\pm$0.7	1.7$\pm$0.4	1.8$\pm$0.2	1.6$\pm$0.4	10.0$\pm$0.7
H_2 S(0)	28.219	4.8$\pm$4.8	$\leq$4.4	$\leq$3.5	$\leq$3.3	$\leq$4.5
Atomic Fine Structure Lines						
SIV	10.510	$\leq$2.3	$\leq$2.9	$\leq$3.1	$\leq$ 1.8	$\leq$1.7
FeII	25.988	$\leq$2.3	$\leq$2.0	$\leq$1.4	$\leq$2.1	$\leq$2.2
SIII	33.480	$\leq$3.3	$\leq$6.6	$\leq$8.3	$\leq$1.7	$\leq$3.3
SiII	34.814	3.4$\pm$1.3	4.7$\pm$0.5	8.6$\pm$0.1	1.8$\pm$0.3	$\leq$3.4

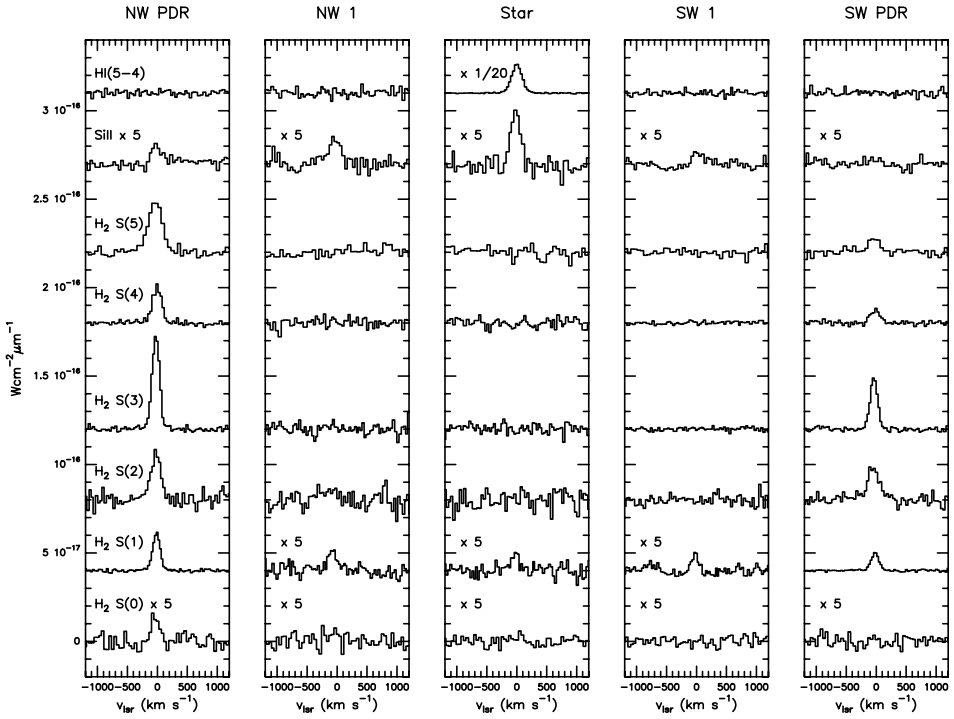

Fig. 2. Spectra of the H_2 S(0),S(1),S(2),S(3),S(4) and S(5) rotational lines, the SiII (34.8 μm) line and the Brα HI recombination line towards the five positions observed across the PDR associated with NGC 7023 (see Fig. 1).

we have plotted in Fig. 3 the normalized intensities of the [HI] 21cm line (Fuente et al. 1996, 1998), the H_2 S(1) v=0–0 and [SiII] 34.8 μm lines as a function of the distance from the star.

3.1. Recombination lines

The Brα line has only been detected towards the star. Continuum emission at 3.6 cm and 6 cm was detected by Skinner et al. (1993). They interpreted the emission as arising in an ionized anisotropic wind. Later, Nisini et al. (1995) observed the Paβ, Brγ, Brα, Pfγ and Pfβ recombination lines with an aperture of 10$''$ and modeled the wind with a mass loss rate of 3.9 10^{-7} $M_\odot$ yr^{-1} and a terminal velocity of 280 kms^{-1}. We have measured an intensity of the Brα line of 1.4 10^{-3} erg s^{-1} cm^{-2} sr^{-1} which agrees within the calibration uncertainties with the data of Nisini et al. (1995).

3.2. The CII and OI lines

The [CII] 157.7 μm and the [OI] 63 and 145.6 μm lines have been detected towards all the observed positions. The intensities and line intensity ratios are shown in Table 2. The emission of the three lines is maximum in the NW PDR and decreases towards the south, being the SW PDR fainter by a factor of 2 than the NW

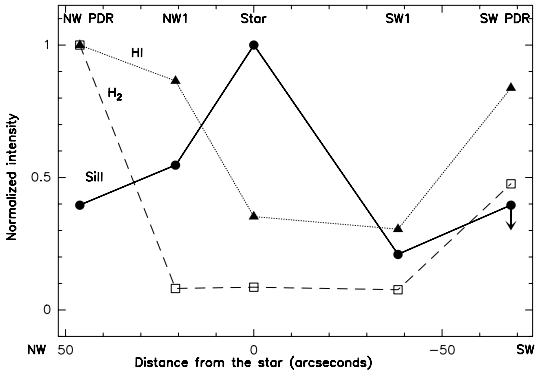

Fig. 3. Normalized intensity of H_2 S(1), HI 21cm and SiII(34.8 μm) lines as a function of the distance from the star. Note that both, the H_2 and HI emission peaks towards the H_2 filaments, while the SiII(34.8 μm) emission peaks towards the star.

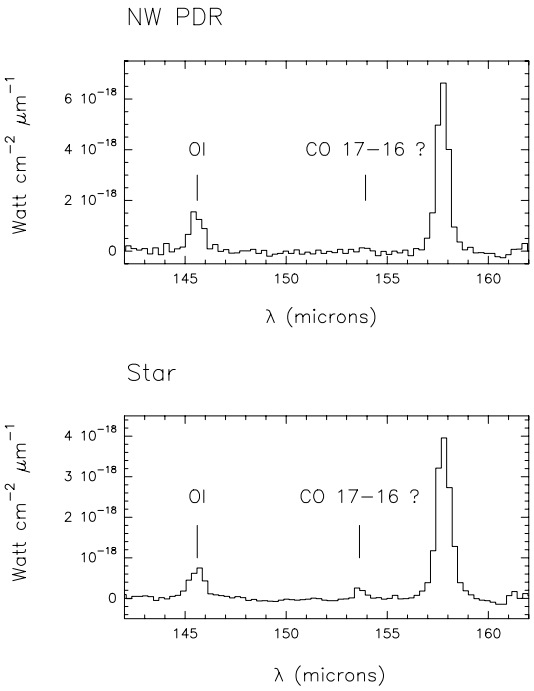

Fig. 4. LWS spectra towards the NW PDR and the star position after subtracting the continuum emission.

PDR. Along the observed strip, the OI(63 μm)/OI(145.6 μm) and OI(63 μm)/CII(157.7 μm) ratios are uniform and take the values $\sim$ 10 and $\sim$ 2 respectively. This means that at the scale of the LWS observations, the physical conditions of the nebula are quite uniform. High angular resolution observations show that this PDR is formed by high density filaments immersed in a more diffuse medium (Sellgren et al. 1992; Lemaire et al. 1996; Fuente et al. 1996). Because of the low angular resolution of the LWS observations, they are very likely tracing the more extended diffuse medium.

3.3. Other ionic and atomic fine structure lines: SiII

The spatial distribution of the SiII line is very different from that of the CII, OI and HI lines (see Fig. 3). While the CII, OI and HI lines peak towards the NW PDR, the SiII line peaks towards the star, with the intensity towards the star $\sim$ 3 times larger than towards the NW PDR. This different spatial distribution cannot be explained by the different angular resolution of the CII and OI observations. The [HI] 21cm line map which has an angular resolution similar to that of the SiII line presents a ring-like morphology with the peaks towards the NW and SW PDRs and a minimum towards the star, just in the peak of the SiII line. The implications of the peculiar spatial distribution of the SiII emission are discussed in Sect. 4.1. We have not detected the [SIII] 33.480 μm, [SIV] 10.51 μm and [FeII] 25.9 μm lines at any position (see Table 3 for upper limits).

3.4. H_2 rotational lines

We have observed the v=0–0 H_2 rotational lines from S(0) to S(5) towards the positions shown in Fig. 1. The intensities of the H_2 lines for all positions are shown in Table 2. Towards the positions NW1, SW1 and the star, we have detected only the S(1) line which prevents from any excitation analysis. The most intense H_2 emission is found towards the NW and SW PDRs. These positions are spatially coincident with the filaments observed in H_2 fluorescent emission which are located in the interface between the atomic and the molecular gas. The H_2 emission is much weaker towards the HI clump (position NW1) and the SW1 position, suggesting that this region is mainly atomic. In contrast with the spatial distribution of HI which is more intense towards NW1 than towards SW1, the spatial distribution of the H_2 emission is quite symmetric around the star.

3.5. Molecular lines

Several molecular lines of species that are expected to be abundant in PDRs (CO,OH,CH,CH_2,H_2O) have observable lines in the wavelength range covered by the LWS01 spectrum. In the LWS01 spectrum towards NW PDR we have tentatively detected a weak line centered at 153.927 μm with a S/N ratio of $\sim$ 3. A weak line centered at 153.637 μm with a S/N ratio of 5 appears also in the spectrum towards the star. Both spectra are shown in Fig. 4. Taking into account that the spectral resolution of the LWS at these frequencies is 0.6 μm, both lines can be identified with the CO J = 17$\rightarrow$16 line (153.267 μm). However, since other CO lines have not been detected towards these positions, we cannot discard the possibility of a misidentification or a spurious detection. Towards the SW PDR, we have not detected any molecular line with typical upper limits of $\sim$ 5 10^{-12} - 5 10^{-13} erg s^{-1} cm^{-2} μm^{-1} depending on the detector being the best limits for detectors 8 to 9 (161.2 to 196.7 μm).

4. Discussion

The NW PDR was modeled for the first time by Chokshi et al. (1988) with an incident UV field of G_0=2.4 10^3 and a density of n = 10^4 cm^{-3}. Models of this region based on H_2 ro-vibrational lines (Martini et al. 1997), CO, CI and CII lines (Gerin et al.

1998) and H_2 rotational lines (Fuente et al. 1999) give slightly higher values of the UV field, G_0= 10^4, and density, n = 10^5 – 10^6 cm^{-3}. We can estimate the UV field and density of the PDR based on the observed OI and CII lines. Along the observed strip, the OI(63 μm)/OI(145.6 μm) ratio is $\sim$ 10. This value is lower by a factor $\sim$ 2-3 than those predicted by PDR models for a region with a UV field of 10^3 and a density of $\sim$ 10^4 cm^{-3} (see e.g. Kaufman et al. 1999; Burton et al. 1992 and references therein). Low OI(63 μm)/OI(145.6 μm) ratios have been observed towards other PDRs and interpreted as the consequence of the self-absorption of the 63 μm line by the foreground gas (Lorenzetti et al. 1999). This interpretation is not plausible for our region in which the extinction by the foreground dust is < 2 mag (Fuente et al. 1998; Gerin et al. 1998). We have no explanation for the low observed values of the OI(63 μm)/OI(145.6 μm) ratio.

Because the [OI] 63 μm and [CII] 157.7 μm lines have different critical densities, the OI(63 μm)/CII(157.7 μm) ratio constitute a good density tracer for densities 10^3 - 10^6 cm^{-3}. The value of the OI(63 μm)/CII(157.7 μm) is $\sim$ 2 towards all the observed positions. This value is consistent with model predictions for G_0 $\sim$ 10^3 and n $\sim$ 10^3 – 10^4 cm^{-3} which are the physical parameters derived by Chokshi et al. (1988) from the same lines and better angular resolution observations. Densities around 10^4 cm^{-3} are also derived from the rotational lines of CO and its isotopes (Fuente et al. 1993; Rogers et al. 1995; Gerin et al. 1998) and from the VLA HI observations (Fuente et al. 1993, 1998). However, densities as high as n = 10^6 cm^{-3} are derived from the H_2 ro-vibrational and rotational lines (Lemaire et al. 1996; Martini et al. 1997; Fuente et al. 1999; this work). High densities (n = 10^5 cm^{-3}) are also derived from the observations of molecular lines towards the NW PDR (Fuente et al. 1993, 1996). As commented in Sect. 3.2, this PDR is formed by high density filaments immersed in a more diffuse medium. The observed OI(63 μm)/CII(157.7 μm) ratio is very likely determined by the value of this ratio in the diffuse component, n $\sim$ 10^4 cm^{-3}, which fills most of the LWS aperture. In fact, the better angular resolution [CII] 157.7 μm and [OI] 63 μm data reported by Chokshi et al. (1988) and Gerin et al. (1998) show that the emission of both lines is extended over the whole HI region. The high density filaments (n $> 10^5$ cm^{-3}) are better traced by the observations of the H_2 rotational and ro-vibrational lines towards the NW and SW PDRs, as well as by the observation of the rotational lines of molecules with high dipole moment.

4.1. SiII

The emission of the [SiII] 34.8 μm line is considered to arise mainly in the neutral part of the cloud, i.e., in the PDR. Silicon has a first ionization potential of 8.15 eV and remains singly ionized until an optical depth of $A_v \sim 5$, a value which is fairly independent of n and G_0. With a critical density of n = 3.4 10^5 cm^{-3}, the intensity of the [SiII] 34.8 μm line is strongly dependent on the uncertain Si abundance in gas phase. Silicon is heavily depleted in the ISM with logarithmic depletion values (δ_{Si} = log(X_{Si}^{gas}/X_{Si})) ranging from -1.30 to -0.18. Most PDR models adopt an Si abundance of 3.6 10^{-6} (δ_{Si}= -1.0) which is the mean value derived by van Steenberg & Shull (1988) but the actual value in the PDR could differ by an order of magnitude, and consequently the intensity of the [SiII] 34.8 μm line. The [SiII] 34.8 μm line is usually compared with the [OI] 63 μm line because both lines have similar excitation conditions and their total column densities are fairly independent of n and G_0. Standard PDR models (δ_{Si}= -1.0) predict SiII(34.8 μm)/OI(63 μm) intensity ratios ranging from $\sim$ 0.06 - 0.08 for G_0 = 10^3 - 10^4 and densities $\sim$ 10^4 - 10^5 cm^{-3} (e.g., Burton et al. 1992).

As it is shown in Figs. 2 and 3, the spatial distribution of the SiII emission in NGC 7023 is different from that of all the other PDR tracers. All the PDR tracers peak towards the vibrationally excited H_2 filaments located in the walls of the cavity in which the star is immersed (the NW and SW PDRs) while the SiII emission fills this cavity and peaks towards the star. The intense H_2 filaments observed towards the NW and SW PDRs show that the extinction from the star to these positions is lower than 2 mag. Then, the SiII emission is arising in the gas located at an extinction of < 2 mag from the star.

We have compared the SiII data with the OI observations reported by Chokshi et al. (1988) which have a FWHM aperture of 33″. Chokshi et al. (1988) measured an intensity of 1.2 $\pm$ 0.1 10^{-3} erg s^{-1} cm^2 sr^{-1} towards the NW PDR. The SiII(34.8 μm)/OI(63 μm) intensity ratio is 0.03 at this position. This value is in agreement with PDR models if the assumed Si elemental abundance is $\sim$ 1.5 10^{-6} (δ_{Si}= -1.3), i.e., silicon is heavily depleted with only the 5% in gas phase. Chokshi et al. (1988) observed a position shifted 20″ W from the star and measured an intensity of 6.2$\pm$0.1 10^{-4} erg cm^{-2} s^{-1} sr^{-1}. Taking into account the dust and gas distribution around the star (see Fig. 1), this value can be considered an upper limit to the actual OI emission and we can conclude that the SiII (34.8 μm)/OI (63 μm) line ratio is > 0.14 towards the star, i.e. a factor of 4 larger than towards the NW PDR. If the SiII emission arise mainly in neutral gas, the Si abundance in gas phase must be larger by more than a factor of 4 towards the star than towards the NW PDR, i.e. at least 20% of the silicon is in gas phase towards the star.

Even more suggestive is to compare the SiII with HI emission. The SiII/HI ratio presents a symmetric distribution around the star, in which the SiII/HI ratio increases towards the star and is a factor of 7 larger towards the star than towards the NW and SW PDRs. If the SiII arise in the mainly neutral layer traced by HI, more than 30% of the Si is in gas phase towards the star. Another possibility is that an important fraction of the SiII emission arise in ionized gas which is not traced by the HI emission. The contribution of the ionized wind to the intensity of the SiII line is expected to be negligible. We have carried out some model calculations using the code CLOUDY[1] (Ferland 1996) assuming the Kurucz stellar atmosphere for a star with T_{eff} = 17000 K, log g=4 cm^{-2} (Kurucz 1979) and the wind parameters derived by Nisini et al. (1995). These calculations show that even assuming the solar abundance for silicon, the SiII intensity in the ionized wind is expected to be a factor of 10^{-7} lower than the intensity of the Brα line. Alternatively, the SiII emission could

arise in a small HII region created by the star. The SiII intensity in an ionized sphere around the star with constant density, n = 10^2 cm^{-3}, could be as high as 3.2 10^{-5} erg s^{-1} cm^{-2} sr^{-1} if all the silicon is in gas phase, i.e., $\approx$ 40% of the SiII emission towards the star. In this case only the 60% of the emission observed towards the star would arise in the neutral layer traced by HI. But even in this case the Si abundance in the neutral gas must increase by a factor of 4 to explain the SiII/HI ratio.

Then we can conclude that silicon is heavily depleted for $A_v \geq$ 2 mag (δ_{Si}= -1.3) and its abundance increases progressively towards the star where at least 20% – 30% of the silicon must be in gas phase.

At this point, it is interesting to consider the case of the [FeII] 26.0 μm line. We have not detected the emission of the [FeII] 26.0 μm line towards any position. This lack of emission can be explained by excitation effects and a different depletion of Fe and Si on grains. The critical density of the [FeII] 26.0 μm line is an order of magnitude larger than that of the [SiII] 34.8 μm line (Hollenbach & Mc Kee 1979). On the other hand, Si is more easily released to the gas phase than Fe. Fe is expected to be significantly depleted in the HII region and the PDR although the Si has been released to the gas phase (Sofia et al. 1994). In standard PDR models, the depletion of Fe is assumed to be a factor of 10 larger than that of Si (δ_{Fe}= -2.0) and the intensity of the FeII(26.0 μm) lines is then an order of magnitude lower than the intensity of the SiII (34.8 μm) line (Burton et al. 1992).

It is well known that the abundance of gas phase silicon in the interstellar medium increases by grain-grain collisions and/or sputtering in shocks (Martín-Pintado et al. 1992, Caselli et al. 1997; Bachiller & Pérez-Gutierrez 1997). Photodesorption of Si in grain mantles by UV radiation has recently been proposed as a mechanism to explain the large SiO abundance in some PDRs (Walmsley et al. 1999). Our data put some constraints on the efficiency of photodesorption to release Si to the gas phase. In NGC 7023, Si is heavily depleted (δ_{Si}= -1.3) in gas at an extinction of 2 mag, i.e., silicon is mainly in solid form in the molecular gas where the emission of SiO is expected to arise. The large bipolar cavity associated with HD 200775 proves the existence of an energetic bipolar outflow in a previous stage of the stellar evolution (Fuente et al. 1998). The large gas phase Si abundance in the positions closest to the star could be a relique of this stage. If it were the case, the efficiency of photodesorption to return the Si to the gas phase would be even lower.

4.2. A gradient in the ortho-to-para-H_2 ratio

The S(0),S(1),S(2), S(3), S(4) and S(5) v=0–0 H_2 rotational lines have been detected towards the NW PDR and the S(1),S(2), S(3), S(4) and S(5) lines towards the SW PDR. In a previous paper (Fuente et al. 1999), we have studied in detail the H_2 rotational lines towards the NW PDR. In this paper we will concentrate in the observations towards the SW PDR.

[1] We have used the version number 90.04 which uses the MICE interface developed by Henrik Spoon at MPE

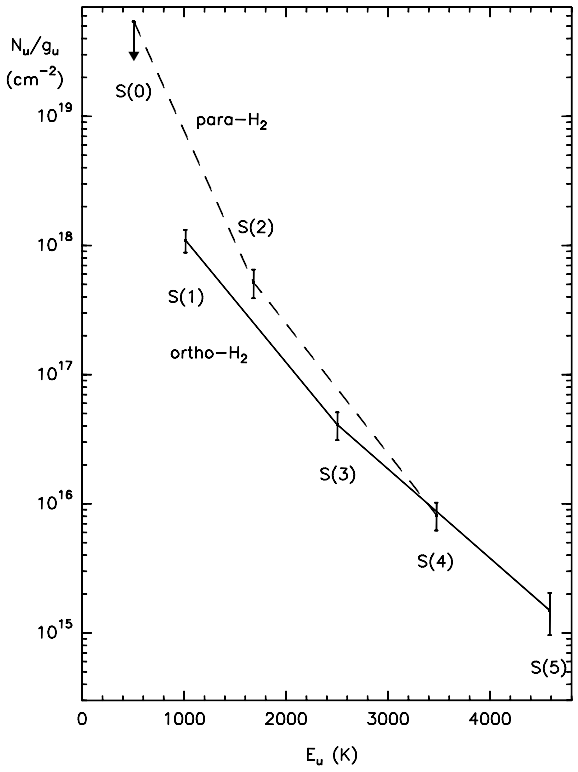

Fig. 5. Rotational diagram of the pure H_2 rotational lines observed towards the SW PDR. The points corresponding to para-levels are joined by a dashed line, and the points corresponding to ortho-levels with a thick line. Note that there is a shift between the ortho- and para-H_2 lines that is larger than the observational errors.

In Fig. 5 we show the rotational diagram of the H_2 lines towards the SW PDR. Note that the errors in Fig. 5 are entirely dominated by the calibration uncertainties (15% at 6.909 μm, 25% at 8.025 μm, 25% at 9.665 μm, 25% at 12.279%, 20% at 17.035 μm and 30% at 28.219 μm). The data have been corrected for dust attenuation using the value for the dust opacity derived from the LWS01 spectra (A_v = 0.3 mag) and the extinction curve of Draine & Lee (1984). The extinction for the S(0), S(1), S(2), S(3), S(4) and S(5) lines amounts to 0.006,0.013, 0.013, 0.027,0.013 and 0.006. Like in the case of the NW PDR (see Fuente et al. 1999), the rotational diagram of the SW PDR shows that the ortho-H_2 levels have systematically lower N_u/g_u values (where N_u and g_u are the column densities and degeneracies of the upper levels of the transitions) than the adjacent J-1 and J+1 para-H_2 levels producing a "zig-zag" distribution. In fact, the ortho-levels seem to define a curve which is offset from that of the para-levels by more than a factor of 2 (see Fig. 5). This offset cannot be explained by calibration uncertainties and extinction effects. The calibration uncertainties are at most 30%. Since the values of the extinction at 17.03 μm, 12.3 μm and 8.025 μm are very similar (Draine & Lee 1984), a correction for dust attenuation cannot push the S(1), S(2) and S(4) points to the same curve. This "zig-zag" distribution cannot be due to the different apertures of the instrument for the different lines. In the case of a point-like source, the S(1) and S(2) lines should

be corrected by a factor 1.35 relative to the S(3) line and the offset between ortho- and para- curve would increase.

The "zig-zag" distribution observed in the rotational diagram can only be fitted by assuming a non-equilibrium OTP ratio, i.e., different from the OTP equilibrium value at the gas kinetic temperature. In this case, only the rotation temperature between the levels of the same symmetry constitute an estimate of the gas kinetic temperature. Using the ortho-levels, we have derived a rotation temperature of $\sim$ 450 K between the S(1) and S(3) lines and of $\sim$ 630 K between the S(3) and S(5) lines. For the para-levels we have derived a rotation temperature of $\sim$ 430 K using the S(2) and S(4) lines. Then we can conclude that the H_2 rotational lines are arising in gas with kinetic temperatures ranging from $\sim$ 400 to 700 K. These kinetic temperatures are similar to those obtained in the NW PDR, but the intensities of the lines are about a factor of 2 lower. A change in the incident UV field and/or the density would imply a variation of both the line ratios (rotation temperatures) and the line intensities. Since the line ratios are similar to those of the NW PDR and the line intensities are significantly lower, we conclude that the SW PDR has the same excitation conditions as the NW PDR ($G_0 = 10^4$, n = 10^6 cm^{-3}) but a beam filling factor of $\sim$ 0.5. All PDR models which include both, chemical and thermal balance in the gas, assume a fixed value of 3 for the OTP ratio, which is the equilibrium value for gas kinetic temperatures $>$ 100 K. In order to determine the value of the OTP ratio in the SW PDR, we have corrected the intensities predicted by the model of Burton et al. (1992) for the effect of different values of the OTP ratio assuming that the total amount of H_2 molecules at each temperature and the line ratios between the levels of the same symmetry remain unchanged. This correction is only valid if the excitation of the H_2 lines is mainly collisional which is the expected case for the low rotational transitions. In Fig. 6, we compare the observational data for the S(0), S(1), S(2) and S(3) transitions with the model for $G_0 = 10^4$, n = 10^6 cm^{-3} and a fixed OTP ratio of 3, and the same model corrected for OTP ratios of 1.5 and 2. We obtain that the rotation diagram of the SW PDR is well fitted with an OTP ratio of 1.5 (see Fig. 6). Martini et al. (1997) derived an OTP ratio of 2.3$\pm$0.5 towards the SW PDR based on the H_2 vibrational lines. Because of the optical depth effects in the excitation of the ortho- and para- H_2 vibrational lines, this value is just a lower limit to the actual value of the OTP ratio (Draine & Bertoldi 1996; Sternberg & Neufeld 1999). Then we can conclude that the OTP ratio is larger than 2.3$\pm$0.5 in the less shielded layers of the PDR ($A_v < 0.7$ mag) where the vibrational lines arises. The gas kinetic temperature in these layers ranges from several hundreds to 2000 K. Comparing the OTP ratio derived from the rotational lines with that derived from the vibrational lines, we conclude that the OTP ratio increases across the PDR. It takes values $\sim$ 1.5 at temperatures of $\sim$ 400 - 700 K and values close to 3 at temperatures $\gtrsim$ 700 K.

The same behavior, a non-equilibrium OTP ratio for the gas with kinetic temperatures $\sim$ 400 K and a gradient of the OTP ratio across the PDR was found in the NW PDR by Fuente et al. (1999). They discussed that the most likely explanation for this behavior is the existence of an advancing photodissociation front. An important problem remains in this explanation, the velocity of the photodissociation front required to have a non-equilibrium OTP ratio is too large ($\sim 5\ 10^5$–$10^7 n^{-1}$ kms^{-1}). However, since the expected behavior of the OTP ratio in an advancing photodissociation front is in agreement with that observed in our data (the cooler gas is further from the OTP equilibrium value than the warm gas) and there are many uncertainties in this estimate (it is not known the OTP ratio at which the H_2 is formed within the PDR, the gas is clumpy and small dense clumps can be evaporating into the PDR,...), we considered that this was the most likely explanation. Later, Lemaire et al. (1999) have obtained a very high spectral resolution spectrum of the H_2 S(1) v=1$\rightarrow$0 line at 2.121 μm towards the NW PDR. The H_2 line is seen shifted in velocity relative to that of the HI and the CO rotational lines. They argue that this velocity difference is a clear proof of the presence of dynamical effects in this PDR and estimated a (projected) velocity of 1 kms^{-1} for the photodissociation front. So far, very few models have been developed for non-equilibrium PDRs (Bertoldi & Draine 1996; Störzer & Hollenbach 1998). These models consider regions illuminated by O stars in which a ionization front is combined with a photodissociation front and assume a fixed value for the OTP ratio

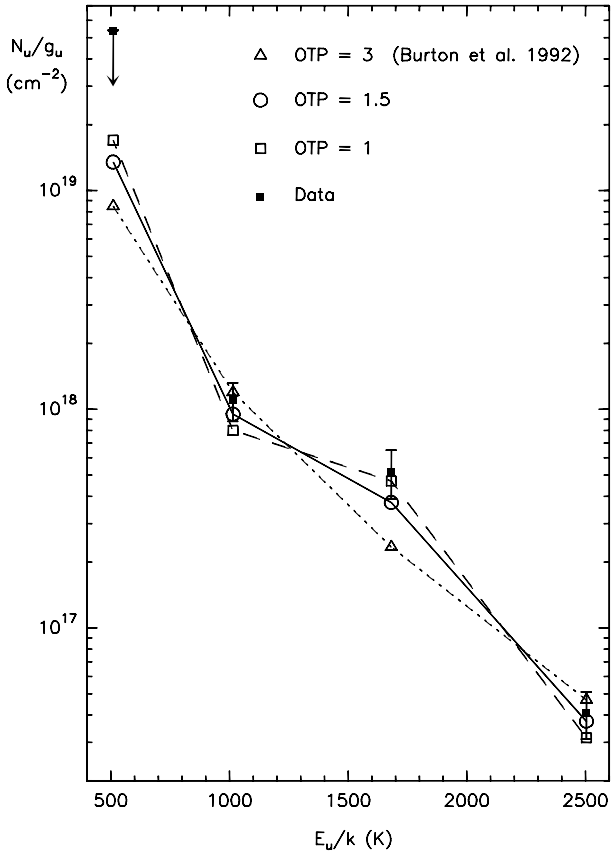

Fig. 6. Comparison of the observational data with the results of PDR models with $G_0 = 10^4$, n = 10^6 cm^{-3}, and OTP ratios of 3 (open triangles), 1.5 (open circles) and 1 (open squares). The data are shown with black squares and errorbars. The beam filling factor has been taken 0.5 for all the models. The model with OTP = 1.5 fits the observational data.

of 3. They do not give any information about the effect of an advancing photodissociation on the ortho-to-para- H_2 ratio. But they predict how the existence of a photodissociation front affects the thermal structure of the region. Following the model by Störzer & Hollenbach (1998), because of the advection of molecular gas through the PDR, the intensities of the H_2 rotational lines and vibrational lines can be enhanced by a factor of 3. Assuming a velocity of 1 kms^{-1} for the photodissociation front, the intensities of the H_2 rotational lines observed in the NW PDR can be well fitted with a density of n$\sim 10^5$ cm^{-1} and a UV field of $G_0 = 10^4$. A non-equilibrium OTP ratio has to be assumed to explain the "zig-zag" distribution.

4.3. Absence of molecular emission

Towards NW PDR we have tentatively detected a weak line centered at 153.927 μm with a S/N ratio of ~ 3. A weak line centered at 153.637 μm appears also in the LWS spectrum towards the star position with a S/N ratio of 5. Taking into account that the spectral resolution of the LWS at these frequencies is 0.6 μm, both lines can be identified with the CO J = 17$\rightarrow$16 line (153.267 μm). However, since other CO lines have not been detected towards these positions, we cannot discard the possibility of a misidentification or a spurious detection. If confirmed, this line would implied the existence of a gas with $T_k >$ 200 K and n$> 10^5$ cm^{-3} in the vicinity of the star. However the density of the bulk of the molecular gas in the PDR must be at least an order of magnitude lower. Federman et al. (1997) estimated based on the ultraviolet absorption lines of CH, CH^+, C_2 and CN that the density of the PDR in front of the star is $\sim$ 200 cm^{-3}. Furthermore, the OI(63 μm)/CII(157.7 μm) ratio is consistent with densities of 10^4 cm^{-3}.

We have not detected any OH, CH and CH_2 line towards the observed positions. Emission of the OH lines have been detected in several sources (NGC 7027: Liu et al. 1996; R CrA and LkHα 234: Giannini et al. 1999). ISO-LWS observations towards a sample of 11 Herbig Ae/Be stars shows that the OH lines are only detected towards the stars associated with with the largest mean densities (n$> 10^5$ cm^{-3}) as derived from the OI(63 μm)/CII(157 μm) ratio. The non-detection of OH in this nebula is consistent with the idea that the bulk of the molecular gas is formed by the low density component traced by the OI(63 μm)/CII(157.7 μm) ratio.

A similar situation is found for CH and CH_2. Large CH column densities have been detected in absorption. The data by Federman et al. (1997) shows that the CH column density in front of HD 200775 is 3.2$\pm$0.2 10^{13} cm^{-2}. Even if we assume excitation temperatures as low as T_{ex} = 20 K, we should have detected intensities of the order of 10^{-9} erg s^{-1} cm^{-2} for the 180.93 and 149.09 μm lines. The non-detection of these lines can only be explained invoking the excitation conditions. The beam filling factor of the dense gas (n$> 10^5$ cm^{-3}) is very low. Another possibility is that the CH abundance decreases for high densities. This would also explain the lack of CH emission in other sources. In fact, far to our knowledge, emission of CH has not been detected towards any source (just a tentative detection towards NGC 7027).

5. Summary: a model for the nebula

In this paper we present the ISO-SWS and LWS observations towards a strip crossing the star and the most intense PDRs in the reflection nebula NGC 7023. These observations altogether with previous maps in molecular lines and the [HI] 21cm line have allowed to figure out a model of the nebula.

We can consider the nebula as composed by three different regions. The first one is formed by the star, the small HII region around it and the low density gas filling the cavity. Federman et al. (1997) based on studies of absorption lines derived that the density of the gas in front of the star is of a few 10^2 cm^{-3}. A slightly larger value, n = 10^3 cm^{-3}, was found by Gerin et al. (1998) based on observations of the CO rotational lines towards the star. The Brα and [SiII] 34.8 μm lines peak in this region but the [HI] 21cm and H_2 rotational lines have a minimum in emission. The Brα emission is well explained as arising in the stellar ionized wind modeled by Nisini et al. (1995). However, the contribution of the stellar wind to the intensity of the [SiII] 34.8 μm line is expected to be negligible. The [SiII] 34.8 μm line is better explained as arising in the diffuse gas filling the cavity in which at least 20% – 30% of the silicon is in gas phase.

The second region is formed by the walls of the cavity in which the star is immersed. Clumpy PDRs have been formed in these walls with high density filaments (n $\sim 10^5 - 10^6$ cm^{-3}) immersed in a more diffuse medium(n $\sim 10^4$ cm^{-3}). These high density filaments are located almost symmetrically $\sim 50''$ NW and $\sim 70''$ SW (NW PDR and SW PDR) from the star and constitute the peaks of the [CII] 157.7 μm, [OI] 63.2 and 145.6 μm, [HI] 21cm and H_2 rotational lines emission. The NW and SW PDRs have very similar excitation conditions although the SW PDR is a factor of 2 weaker than the NW PDR. This difference in intensity is very likely due to a different beam filling factor. In both, the NW and SW PDRs, the intensities of the H_2 rotational lines can only be fitted assuming an ortho-to-para-H_2 ratio lower than 3. Since the rotation temperatures of the H_2 lines ranges from 400 to 700 K, this implies the existence of a non-equilibrium OTP ratio in the region. The comparison between the vibrational and pure rotational H_2 lines suggests that the OTP ratio increases across the PDR from values as low as $\sim$ 1.5 for gas with temperatures $\sim$ 400 – 700 K to values close to 3 in the gas located at a visual extinction $A_v < 0.7$ mag ($T_k \gtrsim$ 700 K). This non-equilibrium OTP ratio has been interpreted in terms of an advancing photodissociation front. The intensity of the [SiII] 34.8 μm line observed towards the NW PDR is consistent with the predictions of PDR models with a standard silicon depletion of δ Si = -1.3, i.e., only 5% of the silicon is in gas phase in these PDRs.

The third region is the molecular gas. We have not detected the OH, CH and CH_2 molecular lines towards this source. This is consistent with the weakness of these lines in other sources and reveals that the beam filling factor of the dense gas (n $\geq 10^5$ cm^{-3}) in the LWS aperture is low. The

CO J=17→16 line has tentatively been detected towards the star.

Acknowledgements. We would like to thank the referee F. Bertoldi for his helpful comments and suggestions. We are also grateful to J. Black for fruitful discussions on the chemistry of this region. This work has been partially supported by the Spanish DGES under grant number PB96-0104 and the Spanish PNIE under grant number ESP97-1490-E. N.J.R-F acknowledges Consejería de Educación y Cultura de la Comunidad de Madrid for a pre-doctoral fellowship.

References

Bachiller R., Pérez-Gutierrez M., 1997, ApJ 487, L93
Bertoldi F., Draine B.T., 1996, ApJ 458, 222
Burton M.G., Hollenbach D.J., Tielens A.G.G.M., 1992, ApJ 399, 563
Caselli P., Hartquist T.W., Havnes O., 1997, A&A 322, 296
Clegg P.E., Ade P.A.R., Armand C.,1996, A&A 315, L38
Chokshi A., Tielens A.G.G.M., Werner M.W., Castelaz M.W., 1988, ApJ 334, 803
de Graauw T., Haser L.N., Beintema D.A., 1996, A&A 315, L49
Draine B.T., Lee H.M., 1984, ApJ 285, 89
Draine B.T., Bertoldi F., 1996, ApJ 468, 269
Hollenbach D., McKee C.F., 1979, ApJ 342, 306
Federman S.R., Knauth D.C., Lambert D.L., Anderson B.-G., 1997, ApJ 489, 758
Ferland G.J., 1996, Hazy, a Brief Introduction to Cloudy. University of Kentucky, Department of Physics and Astronomy, Internal Report
Fuente A., Martín-Pintado J., Cernicharo J., Brouillet N., Duvert G., 1992, A&A 237, 471
Fuente A., Martín-Pintado J., Cernicharo J., Bachiller R., 1993, A&A 276, 473
Fuente A., Martín-Pintado J., Neri R., Rogers C., Moriarty-Schieven G., 1996, A&A 310, 286
Fuente A., Martín-Pintado J., 1997, ApJ 477, L107
Fuente A., Martín-Pintado J., Rodríguez-Franco A., Moriarty-Schieven G.D., 1998, A&A 339, 575
Fuente A., Martín-Pintado J., Rodríguez-Fernández, N.J., et al., 1999, ApJ 518, L45
Gerin M., Phillips T.G., Keene J., Betz A.L., Boreiko R.T., 1998, ApJ 500, 329
Giannini T., Lorenzetti D., Tommasi E., et al., 1999, A&A 346, 617
Kaufman M.J., Wolfire M.G., Hollenbach D., Luhman M.L., 1999, preprint
Kessler M.F., Steinz J.A., Anderegg, 1996, A&A 315, L27
Kurucz R.L., 1979, ApJS 40, 1
Lemaire J.L., Field D., Gerin M., et al., 1996, A&A 308, 895
Lemaire J.L., Field D., Maillard J.P., et al., 1999, A&A 349, 253
Liu X.-W., Barlow M.J., Nguyen-Q-Rieu, et al., 1996, A&A 315, L257
Lorenzetti D., Tommasi E., Giannini T., et al., 1999, A&A 346, 604
Martín-Pintado J., Bachiller R., Fuente A., 1992, A&A 254, 315
Martini P., Sellgren K., Hora J.L., 1997, ApJ 484, 296
Nisini B., Milillo A., Saraceno P., Vitali F., 1995, A&A 302, 169
Rogers C., Heyer M.H., Dewdney P.E., 1995, ApJ 442, 694
Salama A., Feuchtgruber H., Heras A., 1997, ESA SP-419, 17
Sellgren K., Werner M.W., Dinerstein H.L., 1992, ApJ 400, 238
Skinner S.L., Brown A., Stewart R.T., 1993, ApJS 87, 217
Sofia U., Cardelli J.A., Savage B.D., 1994, ApJ 430, 650
Sternberg A., Dalgarno A., 1995, ApJS 99, 565
Sternberg A., Neufeld D., 1999, ApJ 516, 371
Störzer H., Hollenbach D., 1998, ApJ 495, 853
Swinyard B.M., Clegg P.E., Ade P.A.R., 1996, A&A 315, L43
van Steenberg M.E., Shull J.M., 1988, ApJ 330, 942
Walmsley C.M., Pineau de Forêts G., Flower D.R., 1999, ApJ 342, 542